Available online at www.sciencedirect.com

SCIENCE DIRECT®

Composite Structures 67 (2005) 125–133

COMPOSITE STRUCTURES

www.elsevier.com/locate/compstruct

Influence of superposition length on mechanical resistance of single-lap adhesive joints

P.N.B. Reis [a,*], F.J.V. Antunes [b], J.A.M. Ferreira [b]

[a] Dep. Electromecânica, University da Beira Interior, Covilhã 6200, Portugal
[b] Dep. Eng. Mecânica, University de Coimbra, Portugal

Available online 3 August 2004

Abstract

The present work studies the mechanical behaviour of single-lap joints of PP reinforced with glass fibres. Failure loads were obtained experimentally for different superposition lengths (15, 30, 45 and 60 mm). A 2D numerical analysis was developed using the finite element method, and assuming a plane strain state, an orthotropic behaviour for the laminates and an elastic–plastic behaviour for the adhesive. It was found that the positions where σ_{yy} and τ_{xy} stresses have their maximum values, which are near the extremities of the joint and close to the interface adhesive/adherends, move inside the joint with load increasing. An equivalent stress was defined from σ_{yy} and τ_{xy} and was obtained for the failure loads obtained experimentally. This quantity varies 9.7% with superposition length, which can be considered reasonable therefore can be used as a damage criterion for single-lap joints.

Keywords: Single-lap adhesive joints; Composite materials; Finite element method

1. Introduction

Structures made of composite materials are usually a group of individual elements that must be adequately joined. The development of feasible and durable adhesives induced the use of adhesive joints as an alternative to the traditional mechanical joints (bolted, riveted or welded). The adhesive joints reduce stress concentration, are able to join distinct materials and reduce corrosion problems.

The mechanical resistance of adhesive joints must be known to guarantee their integrity in service. The finite element method is an interesting numerical technique to achieve the stress and strain fields of adhesive joints of composite materials. However, the analysis is quite complex due to the heterogeneous and anisotropic behaviour of polymeric materials reinforced with long fibres and different layers; the non-linear and time dependent behaviour of the adhesive; difficulties to obtain the thickness and properties of the adhesive and the geometry of adhesive spew fillet, etc. Moreover, quite refined meshes are usually required with a great number of degrees of freedom.

Several mechanisms can be responsible for the failure of the material, which can grouped in failure of adherends (delamination, failure of the fibres, etc.), failure at the interface adhesive/adherends and failure of the adhesive (cohesive failure). Therefore, different damage criteria have been developed using stress and strain fields to predict limit loads for the adhesive joints. Besides, several parameters influence the mechanical resistance of adhesive joints namely, the materials (fibre, matrix and adhesive, volumetric fraction of fibres, lay-up sequence—combination of ply orientations, stacking sequence—order in which the plies are placed through the thickness, adhesion fibre/matrix), the manufacture procedure (preparation of surfaces to glue, etc.), the geometry of the joint (thickness of the adhesive [1,2] and adherends, superposition length, etc.), loading (loading rate) and environment (temperature, humidity). The single-lap joint is known to be quite sensitive to changes in geometrical parameters [3]. The increase of adherends thickness decreases stress concentration [4]. There is an ideal superposition length, which depends on the adhesive and the adherends [5]. This length gives the best stress distribution, i.e., the lowest stress concentration [4,6].

* Corresponding author. Tel.: +35-127-532-9948; fax: +35-127-532-9972.
E-mail address: reis@dem.ubi.pt (P.N.B. Reis).

0263-8223/$ - see front matter © 2004 Elsevier Ltd. All rights reserved.
doi:10.1016/j.compstruct.2004.01.018

The objectives of this paper are to discuss the superposition length of single-lap joints of PP reinforced with glass fibres using the finite element method to obtain stress and strain fields and to verify the applicability of simple damage criteria to quantify joint failure. A more general work of mechanical behaviour including fatigue strength has been performed [7].

2. Experimental work

The composite plates were obtained with seven lays of two-directional balanced tissue from Vertotex, Twintex T PP, which is a composite material of polypropylene (PP) reinforced with glass fibres type E. The total fibre fraction was 33.4%. These lays were positioned in a mould and submitted to 190 °C and a pressure of 5 bar for 10 min. The plates obtained had a rectangular shape with 160×250 mm and a thickness of 3 mm. The lays were positioned along directions +45/0/−45/0/−45/0/45°, producing a laminated material named +45/0/−45.

These laminated were glued with a cyanoacrylate Super Glue from Bostik reference 7452 Rubber & Plastics grade, after application of a primary Super Glue reference 7480 also from Bostik. Special care was taken on the preparation of adherends to increase adhesion adhesive/composite as polypropylene is a non-polar polymer. The laminates were initially cleaned using ultra-sound and then immersed in a triclorethylene solution for 1 h. The thickness of the adhesive was found to be approximately constant and about 0.1 mm.

The tensile behaviour of adhesive joints was obtained from uniaxial tensile tests at room temperature, according to standard ASTM D5868. The specimens had the geometry indicated in Fig. 1. Four superposition lengths were considered ($L = 15$, 30, 45 and 60 mm), which were loaded up to final failure. The tests were performed using a universal testing machine from Instron, model 4206 and an axial extensometer. Three specimens were tested for each geometry with a strain deformation rate of 0.00333 s^{-1}. Fig. 2 presents the average shear stress-strain curves for each superposition length. The joint with 30 mm superposition length was found to have the highest rigidity and shear strength. The shear strength decreases 41% from 30 to 60 mm, while the strain at failure does not vary significantly.

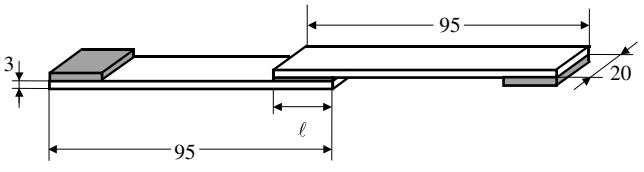

Fig. 1. Geometry of single-lap glued joint.

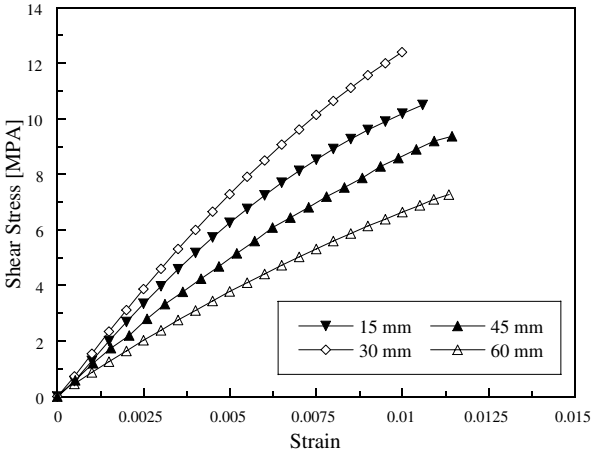

Fig. 2. Shear stress–strain curves for different superpositon lengths.

Table 1
Limit loads

Geometry	ℓ [mm]	P_1 [N]	P_2 [N]	P_3 [N]
$L = 15$ mm	15	3674	3799	4157
$L = 30$ mm	30	8701	8961	9216
$L = 45$ mm	45	8086	8535	10 190
$L = 60$ mm	60	9410	11 580	12 302

Table 1 presents the failure loads, which increase with L, as expected. A specific resistance can be defined ($=P_{max}/(W \cdot L)$, being $W = 20$ mm the width of the joint), which is maximum for $L = 30$ mm and minimum for $L = 60$ mm. The analysis of fracture surfaces indicates that for all superposition lengths studied the damage occurs at the interface fibre/polypropylene, i.e., inside the adherends, as shows the SEM micrography presented in Fig. 3. This type of damage indicates the efficiency of the adhesive and surface treatment used.

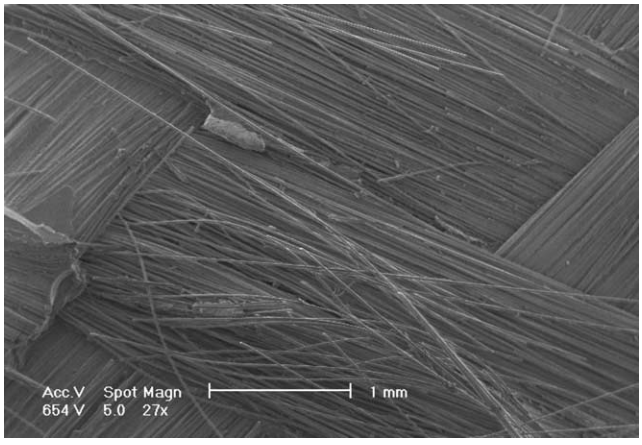

Fig. 3. Fracture surface analysed by SEM micrography.

3. Physical model

The geometry was modelled as a 2D plane strain problem, since the joint is relatively thick (20 mm). This is according the approach followed by different authors [8–13]. Fig. 4 presents the 2D geometry of the adhesive joint. A thickness of 0.1 mm was considered for the adhesive, which was the average value experimentally determined using laser equipment for roughness measurement. In literature most of the studies considered thicknesses within 0.1 and 0.2 mm, although higher values have been considered [14]. This parameter seems to have a significant effect on the stress and strain fields [1,2]. Four superposition lengths were considered (15, 30, 45 and 60 mm), which were loaded up to failure loads indicated in Table 1. The boundary conditions are indicated in Fig. 4 and intend to simulate the restrictions imposed by the grips of the testing machine. Notice that these boundary conditions restrain rigid body movement.

The laminated materials are heterogeneous and anisotropic. However, the adherends were assumed to be continuous, homogeneous and with orthotropic linear elastic behaviour. Although a loss of rigidity with initial damage (microcracks in matrix, failure of fibres, etc.) is expected, according Hildebrand [9], Adams [15] and Charalambides et al. [16] these materials can be modelled as linear elastic. The orthotropic behaviour results from the existence of three orthogonal symmetry planes and reduces the number of elastic constants needed. The main orthotropic directions are indicated in Fig. 5. Table 2 presents elastic orthotropic properties considered in the numerical analysis. The values of E_1 and v_{31} were obtained experimentally from uniaxial tensile tests at room temperature and in air. The specimens were instrumented with extensometers and loaded up to 35% of the material tensile strength, to guarantee an elastic behaviour. The properties along the thickness were assumed to be those of polypropylene, because they are difficult to obtain experimentally. The material was also assumed to have similar properties along x_1 and x_2, which is reasonable considering that it is a balanced tissue.

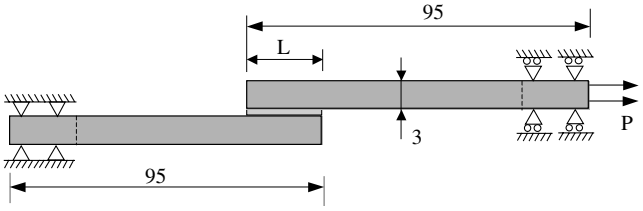

Fig. 4. Physical model for the single-lap glued joint.

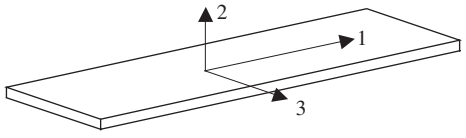

Fig. 5. Principal directions of orthotropic material.

Table 2
Properties of the adherends

Geometry	Value	Comment
E_1 [MPa]	17289.2	Experimental value
E_2 [MPa]	1500	Typical value for PP
E_3 [MPa]	17289.2	$=E_1$
v_{12} [−]	0.32	Typical value for PP
v_{23} [−]	0.028	Considering orthotropic properties
v_{31} [−]	0.125	Experimental value
G_{12} [MPa]	6548.86	$=\frac{E_1}{2(1+v_{12})}$
G_{23} [MPa]	729.57	$=\frac{E_2}{2(1+v_{23})}$
G_{31} [MPa]	768.4	$=\frac{E_3}{2(1+v_{31})}$

The adhesive was assumed to be continuous, homogeneous, isotropic, with elasto-plastic behaviour. In fact, several authors [8,9,11,15,17] recommended a non-linear behaviour for the adhesive. A special specimen was made with the adhesive material to obtain the elasto-plastic behaviour. The elastic properties obtained with a strain rate of 1 mm/min were: $E = 956.44$ MPa, $v = 0.446$. The increase of deformation rate increases Young's modulus and tensile strength but reduces failure deformation [10]. A Ramberg–Osgood equation was fitted to the experimental stress–plastic strain curve:

$$\sigma = 22.9(\varepsilon_p)^{0.186}$$

The adhesive was assumed to obey yield criteria of Von Mises and Prandtl–Reuss flow rule. A kinematic hardening rule was assumed, being the backstress defined by Ziegler's rule.

Four assumptions of this model can introduce analysis errors: to consider a 2D plane strain analysis and to assume a homogeneous behaviour for the adherends, a linear elastic behaviour for the adherends and an elasto-plastic behaviour independent of time for the adhesive.

4. Analysis by the finite element method

The physical model presented in previous section was analysed by the finite element method using commercial finite element package MARC-MENTAT 2000 [18]. The analysis was done assuming large displacements and large strains.

Quadrilateral isoparametric elements with eight nodes were considered. Fig. 6 presents one of the finite element meshes considered, which were refined near the corners where stresses and strains vary significantly. Square elements were considered there because this shape gives best results. Eight elements were considered along the thickness of the adhesive, each with 12.5 μm.

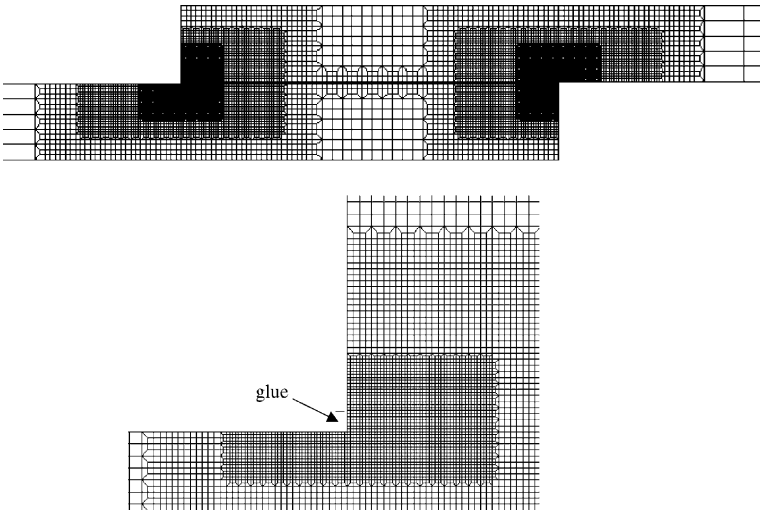

Fig. 6. Finite element mesh for $L = 15$ mm.

Table 3
Total number of nodes and elements

Geometry	Elements	Nodes
$L = 15$ mm	23372	70815
$L = 30$ mm	24388	73901
$L = 45$ mm	25480	77223
$L = 60$ mm	26562	80503

Hildebrand [9] used six quadratic elements and recommended the use of 4–6 elements along the thickness of the adhesive layer to achieve reliable results. Large elements were used far from the corners to reduce the numerical effort involved. Total numbers of elements and nodes are indicated in Table 3.

4.1. Validation of numerical procedure

Fig. 7 presents results for the influence of convergence limit (CL) of Newton–Raphson iterative process. It can be seen that Von Mises equivalent stress obtained at the mid-plane of the adhesive for $L = 45$ mm show irregular results for CL = 1%, which were eliminated with CL = 0.25%. Therefore a value of 0.0075% was considered for CL to avoid these errors. The loading was divided into at least 50 increments, which eliminates the errors associated with exaggerated loading increments.

The sensitivity of stress and strain fields relatively to elastic properties estimated for the adherends was studied. Four values obtained in literature for Poisson's ratio of polypropylene (0.32, 0.34, 0.36 and 0.38) were studied and no influence was found. However, Young's modulus of polypropylene was found to have some influence on stress and strain fields for the range studied (1500, 2000 and 2500 MPa). Fig. 8 presents the influence

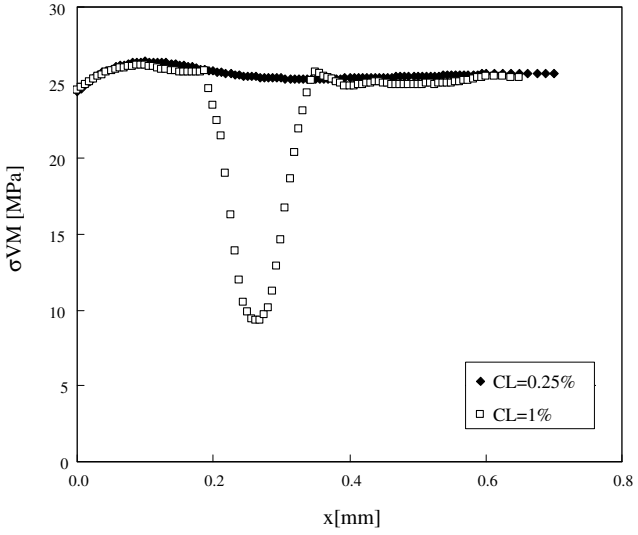

Fig. 7. Influence of convergence limit of Newton–Raphson method on Von Mises equivalent stress ($L = 45$ mm; $y = 0.05$ mm).

of E on principal strain along the mid-line of the adhesive. The influence of this parameter is observed mainly at the extremities of the joint. An increase of 2.8% was observed when E increased from 1500 to 2500 MPa.

Fig. 9 compares experimental load–displacement curves with numerical predictions for $L = 30$ mm. The axial displacement was measured between two points separated 50 mm in both numerical and experimental analysis. A reasonable agreement can be found between the numerical predictions and two of the experimental curves, which is a good indication for the accuracy of numerical results. One experimental curve deviated from the others, the behaviour explained by the scatter typical of experimental testing. The difference between this

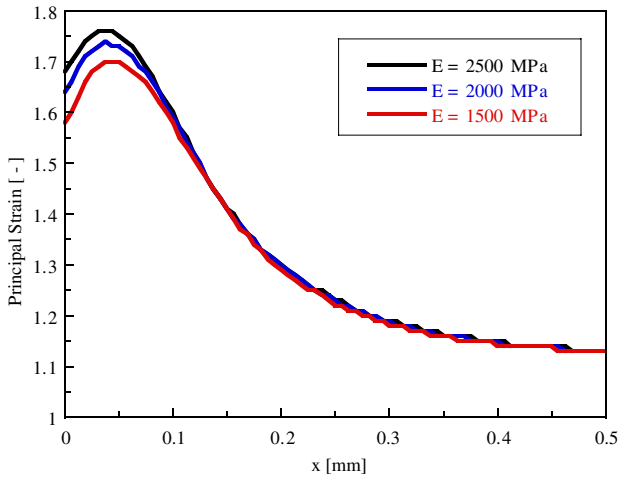

Fig. 8. Influence of E on principal strain along mid-line of the glue.

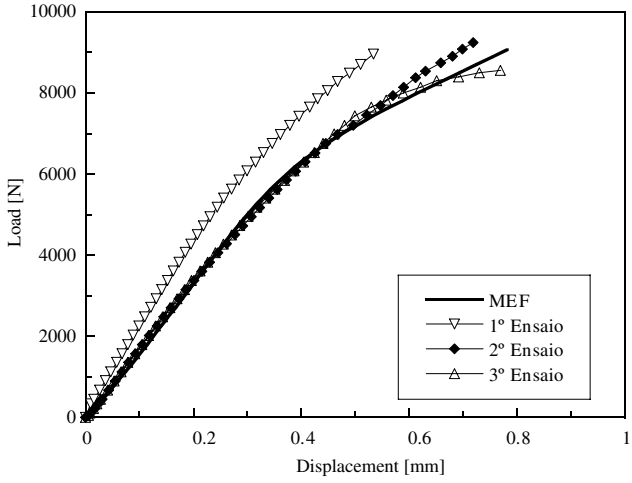

Fig. 9. Experimental load–displacement curves and numerical predictions.

curve and numerical prediction is about 10%. Finally, comparing the numerical with an average experimental curve differences about 2% are obtained, which is acceptable.

Finally, Fig. 10 presents stress distributions along half-thickness of the adhesive obtained with Goland–Reissner [19] and Hart-Smith [20] solutions. Numerical solutions obtained considering linear elastic, linear elastic with geometric non-linearity and elastic–plastic behaviours for the adhesive are also presented. σ_{yy} stresses were normalised by average stress $\tau_{aver} = P/(W \cdot L)$, being $W = 20$ the width of the joint, L the superposition length and P the load. Goland–Reissner and Hart-Smith solutions gave similar stresses, significantly different from numerical results. Similar trends were obtained by Gonçalves [10]. The difference between numerical and analytical results is more significant near the extremities of the joint ($x' = 15$ mm) and lower for an elastic behaviour of the adhesive.

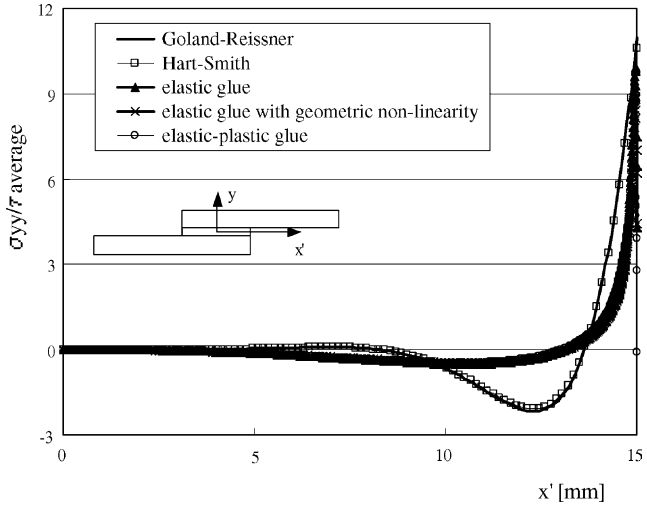

Fig. 10. Comparison of Goland–Reissner and Hart-Smith models with numerical results (stresses along mid-thickness of the glue).

5. Presentation and analysis of results

Fig. 11a presents the deformed shape of adhesive joint (displacements magnified 5×). Fig. 11b presents a detail near one of the corners. The deformation of the adhesive can be seen to be much higher than the deformation of the adherends. This was expected as the adherends were assumed to have an elastic behaviour with relatively high rigidity, while the adhesive was assumed to have an elasto-plastic behaviour with a reduced yield stress. Figs. 12a and b present σ_{yy} and τ_{xy} stress fields, respectively, for a superposition length $L = 30$ mm and a load of 9068 N. The adhesive is not represented in these figures. It can be seen that both adherends have stress concentration regions. For τ_{xy} this concentration is more important at the inferior adherend and near the superposition extremity. A similar behaviour was observed by Ribeiro et al. [21] for epoxy adherends "Biresin L84 TN" and Araldite AW 106 adhesive, using numerical and experimental analysis. Relatively to σ_{yy} field maximum values also occur near the extremities of the joint, which is according the results of Charalambides et al. [16]. The elevated stress values at the extremities of the joint can produce cracks along adhesive/adherent interface or matrix/fibre interface [22]. Once initiated this crack will propagate up to final failure.

5.1. Influence of loading

The influence of loading was studied for a superposition length $L = 30$ mm, to understand the evolution of maximum values of σ_{yy} and τ_{xy} stresses (Fig. 13) as well as their position (Fig. 13). The maximum values were obtained in the adherends along a line at a distance of 25 μm of adhesive/adherend interface. The results of Fig.

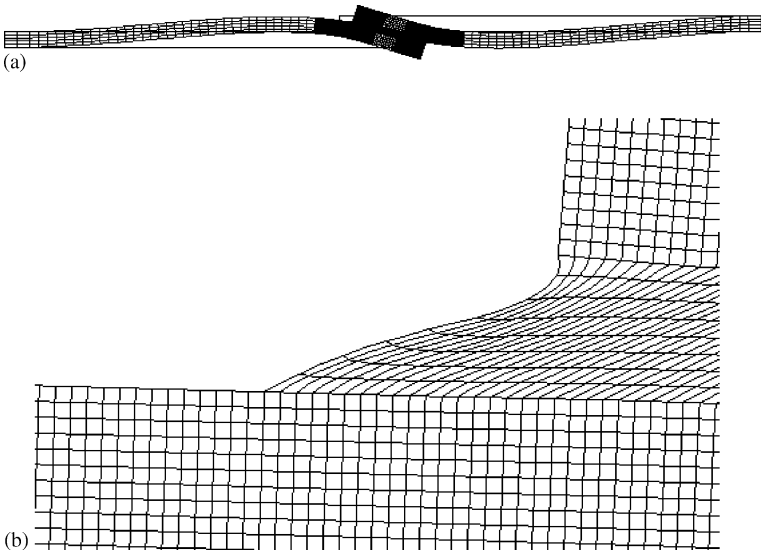

Fig. 11. (a) Deformed shape amplified 5x (geom 1, $P = 4000$ N). (b) Detail of deformed shape (geom 1, $P = 4000$ N).

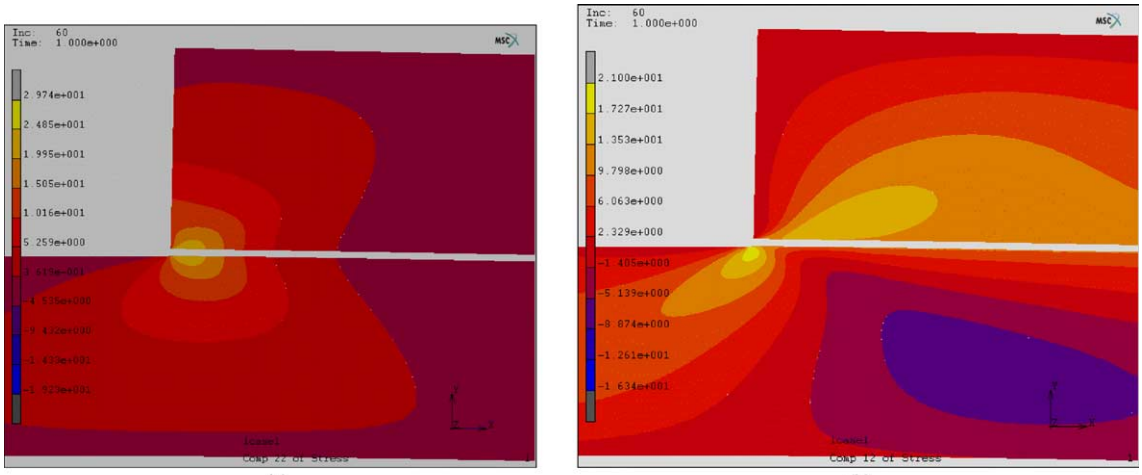

Fig. 12. σ_{yy}, and τ_{xy} stress fields for a superposition length $L = 30$ mm and a load of 9068 N.

13 indicate that the increase of load produce an increase of maximum values of σ_{yy} and τ_{xy}, as expected. Initially these two stresses present similar values, however for loads higher than 2000 N, σ_{yy} increases faster. At failure, for a load of 9068 N, the difference between maximum values of these two stresses is about 40%. The adherends have a linear elastic behaviour therefore a linear variation of σ_{yy} and τ_{xy} could be expected. However, this is not observed due to geometric non-linearity [10] and due to the non-linear behaviour of the adhesive, which is close to measurement points (25 μm). Finally, the important increase of stresses for higher loads can be an indication that final failure is close.

Fig. 14 indicates that σ_{yy} and τ_{xy} stresses have their maximum values at distinct positions, which can be confirmed in Fig. 12. Their positions vary with loading, moving into the interior of the joint. This movement is about 0.5 mm for σ_{yy} stresses and 0.3 mm for τ_{xy} stresses.

5.2. Influence of superposition length

Fig. 15 presents equivalent Von Mises stress along mid-line of the adhesive ($y = 50$ μm) for different superposition lengths and a load of 1000 N. The analysis of this figure indicates that the highest stresses occur close to extremities whatever the superposition length (L). The position of the maximum value does not seem to vary with L. The Von Mises stresses decrease with L, i.e., maximum stresses are obtained for $L = 15$ mm. The difference between maximum values of Von Mises for $L = 15$ mm and 60 mm is about 30%. Minimum values are obtained at the middle point of the joint, being

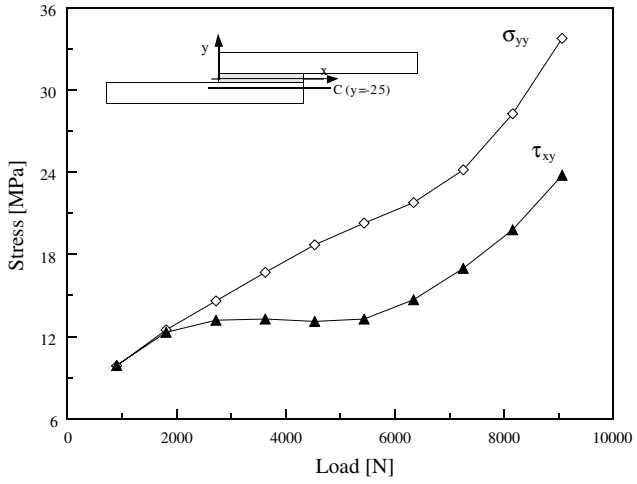

Fig. 13. Evolution of maximum values of σ_{yy}, and τ_{xy} stresses in a superposition length of 30 mm along a line at a distance of 25 μm of adhesive/adherend interface.

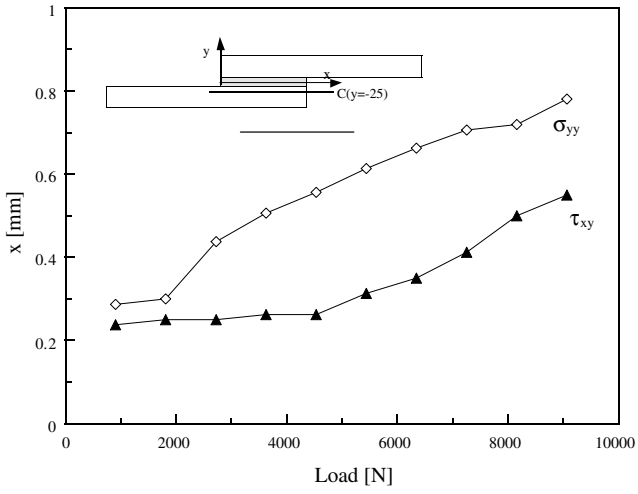

Fig. 14. Evolution of the position of maximum values of σ_{yy}, and τ_{xy} stresses along $y = -25$ μm (superposition length of 30 mm).

about 1 MPa for $L = 30$, 45 and 60 mm, and 2.2 MPa for $L = 15$ mm. Similar trends were obtained for the equivalent plastic deformation along mid-line of the adhesive applying also a load of 1000 N. The highest values are obtained close to the extremities, where the plastic deformation for $L = 15$ mm is one order of magnitude higher than that for $L = 60$ mm.

Figs. 16a and b show the variation of σ_{yy} and τ_{xy} in the adherends, at a distance of 25 μm from adherend/adhesive interface and for a load of 1000 N. Relatively to Fig. 16a it can be seen that for $L \geqslant 30$ mm maximum values of normal stress (σ_{yy}) vary from 7 to 10 MPa and occur close to the extremities of the joint ($x = 0$). The highest value was however obtained for $L = 15$ mm being about 12 MPa, and occurs at a negative value of x. Compressive stresses were obtained at inside points,

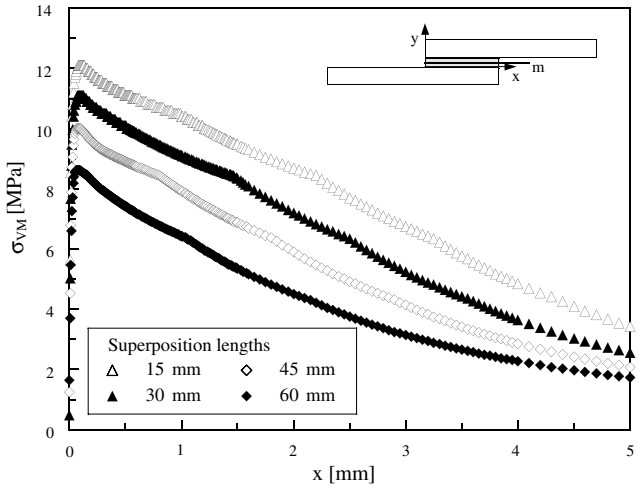

Fig. 15. Equivalent Von Mises stress along mid-line of the adhesive ($y = -25$ μm) for different superposition lengths and a load of 1000 N.

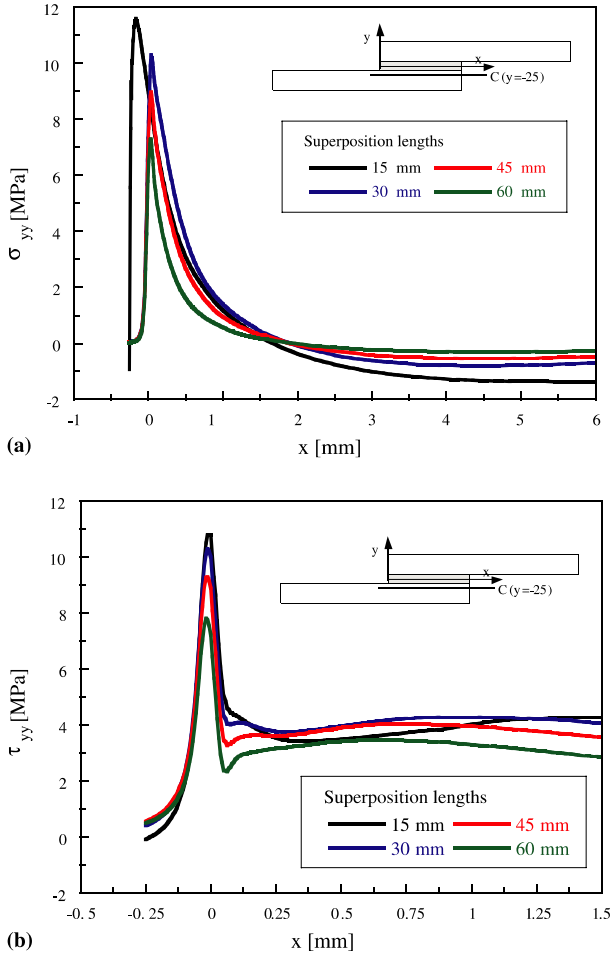

Fig. 16. (a) Variation of σ_{yy} in the adherends at a distance of 25 μm from adherend/adhesive interface for a load of 1000 N. (b) Variation of τ_{xy} in the adherends at a distance of 25 μm from adherend/adhesive interface for a load of 1000 N.

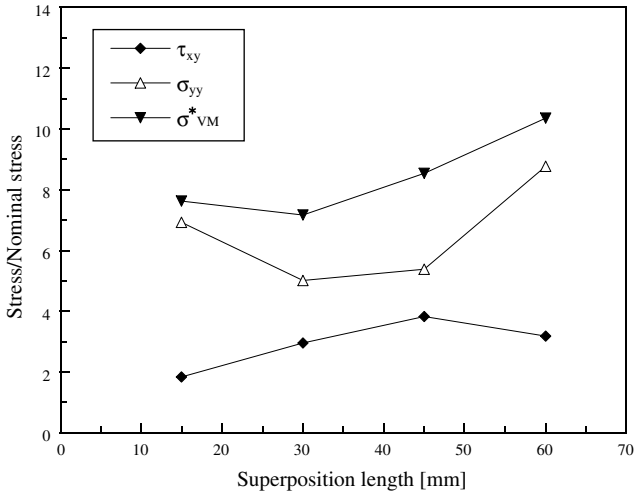

Fig. 17. Effect of the superposition length on maximum values of σ_{yy} and τ_{xy}.

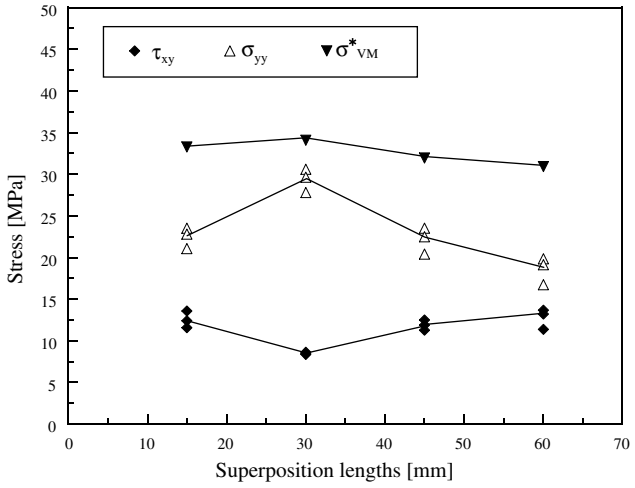

Fig. 18. Maximum values of σ_{yy} and τ_{xy} for the experimental failure loads and the equivalent stress.

with a minimum value of 1.4 MPa for $L = 15$ mm. The analysis of Fig. 16b indicates the presence of maximum values of τ_{xy} close to the extremity of the joint, ranging from 8 to 11 MPa and decreasing with the increase of L.

Fig. 17 presents the effect of superposition length on maximum values of σ_{yy} and τ_{xy} for a load of 1000 N. Both stresses were normalised by average stress $\tau_{aver} = P/(W \cdot L)$. An equivalent stress, based on Von Mises equivalent stress, was defined from σ_{yy} and τ_{xy} according to:

$$\sigma_{eq} = \sqrt{\sigma_{yy}^2 + 3\tau_{xy}^2} \quad (1)$$

The normal stress decreases from $L = 15$ to 30 mm, and increase from this to 60 mm. The shear stress increase up to $L = 45$ mm and decrease to $L = 60$ mm. The equivalent stress increase from $L = 30$ to 60 mm. This trend is according the variation of mechanical resistance obtained experimentally (Table 1). Therefore the numerical results confirm that the superposition length of 30 mm is the best for the adhesive/adherends being studied. According to literature [17,23,24] this length gives the best stress distribution, which is confirmed here by the variation of equivalent stress.

5.3. Analysis of failure

The experimental results indicate that damage occurs in the adherends close to the interface adhesive/adherends (Fig. 3). However it is not possible to identify the exact point where damage initiates. Besides, the numerical analysis of the influence of superposition length (L) indicates that the increase of this distance reduces stress at the adherends. This indicates that failure loads are lower for higher values of L, which is confirmed by experimental results of Table 1.

In order to study the damage criterion more adequate to predict the occurrence of failure, the four superposition lengths were loaded up to failure loads and (σ_{yy}, τ_{xy}) stresses were determined close to the interface adhesive/adherend (at a distance of 25 μm). Fig. 18 presents for each superposition length the maximum values of σ_{yy} and τ_{xy} obtained for the experimental failure loads presented in Table 1. The equivalent stress (Eq. 1) is also presented. The shear stress (τ_{xy}) has a trend opposite to normal stresses (σ_{yy}), decreasing from $L = 15$ to 30 mm and increasing from this to 60 mm. The superposition length of 30 mm presents the highest difference between normal and shear stresses, of about 20 MPa. The equivalent stress varies only 9.7%, which can be considered acceptable. This variation can be explained by the scatter of experimental results and by the simplifications of numerical analysis. Therefore the equivalent stress defined from σ_{yy} and τ_{xy} stresses can be used as a first criterion of damage. However, other models (for example, Tsai–Wu and Tsai–Hill models) should be tested and the numerical analysis must be improved.

6. Conclusions

σ_{yy} and τ_{xy} stresses have their maximum values near the extremities of the joint and close to the interface adhesive/adherends. They present their maximum values at distinct positions, which move to the interior of the joint with increasing load. The superposition length of 30 mm gave a lower equivalent stress, therefore gives the best stress distribution. This equivalent stress, defined from σ_{yy} and τ_{xy} using a modified Von Mises equivalent stress, was obtained for the failure loads obtained experimentally. This quantity varies 9.7% with superposition length, which can be considered reasonable considering the simplifications made to the numerical

analysis and the scatter of experimental failure loads. Therefore these equivalent stresses can be used as a damage criterion for single-lap joints.

References

[1] Burk RC. Standard failure criteria needed for advanced composites. Astronaut Aeronaut 1983;21:58–62.

[2] Ripling EJ, Mostovoy S, Corten H. Fracture mechanics: a tool for evaluating structural adhesives. J Adhesion 1971;3:107–23.

[3] Kairouz KC, Matthews FL. Strength and failure modes of bonded single lap joints between cross-ply adherends. Composites 1993;24(6):475–84.

[4] Lees WA. Stress distribution in-bonded joints: an exploration within a mathematical model. Int J Mater Product Technol 1987;2(2):168–81.

[5] Lee C-C. Determination of the mechanical properties of adhesive for design of bonded joints. PhD thesis. Faculty of Applied Science, School of Materials Science and Engineering, University of New South Wales, Austrália, 1997.

[6] Czarnocki P, Piekarski K. Fracture strength of an adhesive-bonded joint. Int J Adhes Adhes 1986;6(2):93–5.

[7] Ferreira JAM, Reis PNB, Costa JDM, Richardson MOW. Fatigue behaviour of composite adhesive lap joints. Compos Sci Technol 2002;62:1373–9.

[8] Bigwood DA, Crocombe AD. Non-linear adhesive-bonded joint design analyses. Int J Adhes Adhes 1990;10(1):31–41.

[9] Hildebrand M. Non-linear analysis and optimization of adhesively bonded single lap joints between fibre-reinforced plastics and metals. Int J Adhes Adhes 1994;14(4):261–7.

[10] Gonçalves JPM. Contribution for the numerical and experimental analysis of simple lap joints. PhD Thesis. Faculdade de Engenharia, Universidade do Porto, 2000 [written in Portuguese].

[11] Harris JA, Adams RD. Strength prediction of bonded single lap joints by non-linear finite element methods. Int J Adhes Adhes 1984;4:65–78.

[12] Groth HL. Stress singularities and fracture at interface corners in bonded joints. Int J Adhes Adhes 1988;8(2):107–13.

[13] Wang CH, Rose LRF. Compact solutions for the corner singularity in bonded lap joints. Int J Adhes Adhes 2000;20:145–54.

[14] Czarnocki P, Piekarski K. Non-linear numerical stress analysis of a symmetric adhesive-bonded lap joint. Int J Adhes Adhes 1986;6(3):157–60.

[15] Adams RD. Strength predictions for lap joints, especially with composite adherends: a review. J Adhesion 1989;30:219–42.

[16] Charalambides MN, Kinloch AJ, Matthews FL. Adhesively-bonded repairs to fibre-composite materials: II Finite element modelling. Composites Part A 1998;29A:1383–96.

[17] Adams RD, Harris JA. The influence of local geometry on the strength of adhesive joints. Int J Adhes Adhes 1987;7(2):69–80.

[18] MARC User Information. Marc Analysis Research Corp., Palo Alto, 2000.

[19] Goland M, Reissner E. The stresses in cemented joints. J Appl Mech 1944;66:A17–27.

[20] Hart-Smith LJ. Adhesive-bonded single-lap joints. NASA CR-112236, NASA Langley Research Centre, Hampton, Virginia USA, 1973.

[21] Ribeiro JE, Esteves JLS. A photoelastic study of stress field in structural adhesive joints. Mecân Exp 1999;4:41–50 [written in Portuguese].

[22] Abdel Wahab MM. On the use of fracture mechanics in designing a single lap adhesive joint. J Adhes Sci Technol 2000;14(6):851–65.

[23] Lim WW, Mizumachi H. Fracture toughness of adhesive joints. II Temperature and rate dependencies of Mode I fracture toughness and adhesive tensile strength. J Appl Polym Sci 1995;57:55–61.

[24] Vinson JR. Adhesive-bonding of polymer composites. Polym Eng Sci 1989;29(19):1325–31.